

Branching Ratios from B_s and Λ_b^0

Matthew S Martin

CDF Collaboration,

Fermi National Accelerator Laboratory,

MS 318, P.O. Box 500,

Batavia, IL 60510-0500

CDF Run II relative branching ratio measurements for 65 pb^{-1} of data in the channels $B_s \rightarrow D_s^\mp \pi^\pm$, $\Lambda_b^0 \rightarrow \Lambda_c^\pm \pi^\mp$ and $B \rightarrow h^+ h^-$ are presented. Further, an observation of $B_s \rightarrow K^\pm K^\mp$ and a measurement of A_{CP} are presented.

1 Introduction

CDF Run II, and D0 are a unique opportunity to pursue a rich program of B-Physics. Until LHCb or BTeV become operational, CDF and D0 are the only experiments currently taking data that can access the B-baryons and the heavier (than B_d) B-mesons. A precision study of the B_s is currently underway. Branching ratios, mass and lifetime are all being measured. A measurement that would either observe or rule out SM B_s mixing is planned. Measurements of $\Delta\Gamma_{B_s}$ and γ are also envisaged. CDF also has the world's largest Λ_b^0 sample. Branching ratio, mass and lifetime measurements are already underway, or planned in the near future. In the present paper, relative branching ratio results for 65 pb^{-1} of data are presented for the channels $B_s \rightarrow D_s^\mp \pi^\pm$, $\Lambda_b^0 \rightarrow \Lambda_c^\pm \pi^\mp$ and $B \rightarrow h^+ h^-$.

2 Hadronic Level 2 Trigger

The hardware that enables CDF to observe the fully hadronic B signals presented here is the SVT[1] (Second level Vertex Trigger)¹. The interaction rate at CDF is approximately 2.5 MHz . This has to be reduced to a rate of the order 300 Hz to be written to tape. The critical component of the hadronic trigger path are the impact parameter cuts made by the SVT at level 2. The SVT uses the Silicon detector data with the level-1 tracking information from the central tracking chamber. The heart of the algorithm is a parallel look-up operation of previously computed acceptable hit patterns. The legitimate hit patterns are then fed into a Track Fitter stage which gives track parameters curvature, ϕ_0 and most importantly impact-parameter. The two hadronic trigger streams which are implemented at CDF are $B \rightarrow h^+ h^-$ and B-multibody respectively[3]. The impact parameter requirement for the $B \rightarrow h^+ h^-$ stream is two tracks with $d_0 > 100 \mu\text{m}$, while the B-multibody stream requires two tracks with $d_0 > 120 \mu\text{m}$. A plot of the SVT impact-parameter distribution is given in figure 1.

¹The CDF detector is described elsewhere[2]

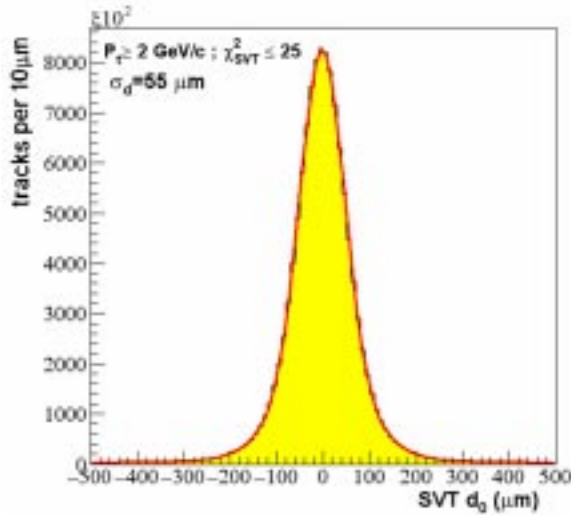


Figure 1: Level 2 SVT impact parameter distribution (μm)

3 Branching Ratios at CDF

At CDF, a branching ratio measurement is quoted as a ratio of branching ratios. For example, in the case of $B_s \rightarrow D_s^\mp \pi^\pm$, the quantity quoted is:

$$\frac{\sigma_b \times f_s \times BR(B_s \rightarrow D_s^\mp \pi^\pm)}{\sigma_b \times f_d \times BR(B_d \rightarrow D^\mp \pi^\pm)} = \frac{\epsilon_{B_d} \times N_{B_s} \times BR(D^- \rightarrow K^- \pi^+ \pi^+)}{\epsilon_{B_s} \times N_{B_d} \times BR(D_s^- \rightarrow \phi \pi^-)} \quad (1)$$

where f_s , f_d are B-meson production fractions, and ϵ_{B_s} , ϵ_{B_d} are total observation efficiencies (trigger and reconstruction). The primary advantage of this is that the systematic uncertainties due to the trigger and reconstruction efficiencies cancel. Furthermore, the b production cross-section cancels. At present, the B-meson production fractions used are the LEP/CDF combined results[4]. However, it is intended that these be measured at CDF Run II. Currently existing measurements are used for the daughter branching ratios. However, it is planned to normalise to the same channel semileptonic modes so that the daughter branching ratios would then cancel.

4 $B_d \rightarrow D^\mp \pi^\pm$

The channel $B_d \rightarrow D^\mp \pi^\pm$ is the normalisation mode for both $B_s \rightarrow D_s^\mp \pi^\pm$ and $A_b^0 \rightarrow A_c^\pm \pi^\mp$. The reconstruction cuts for the normalisation mode are chosen to be as similar as possible to the signal mode cuts (to ensure the best cancellation of systematic errors). For the $B_s \rightarrow D_s^\mp \pi^\pm$ analysis, the selection requirements for the normalisation mode are as follows. First the trigger is confirmed by requiring that 2 of the 4 offline tracks be associated to SVT trigger tracks. Further the p_t , charge, transverse angle, and impact parameter of these offline tracks are required to pass the trigger cuts. The reconstruction cuts are then: [The D^\pm and B_d are reconstructed

using a kinematic fitter]; [The D^\pm mass is constrained to the PDG value]; [$\Delta R(D^\pm \pi_B) < 1.5$ (where π_B is the pion from the B)]; [$\chi_{xy}^{B_d} < 15$, $\chi_{xy}^{D^\pm} < 10$]; [$P_t^{D^\pm} > 4\text{GeV}$, and $P_t^{B_d} > 6\text{GeV}$]; [$L_{xy}^{D^\pm} > 600 \mu\text{m}$, $L_{xy}^{B_d} > 100 \mu\text{m}$ ²]; [The impact parameter for the fully reconstructed B_d meson is required to satisfy $|d_{B_d}| < 100 \mu\text{m}$] The invariant mass distribution obtained can be seen in figure 2. The smaller structure on the left is due to the mode $B_d \rightarrow D^{*-} \pi^+$.

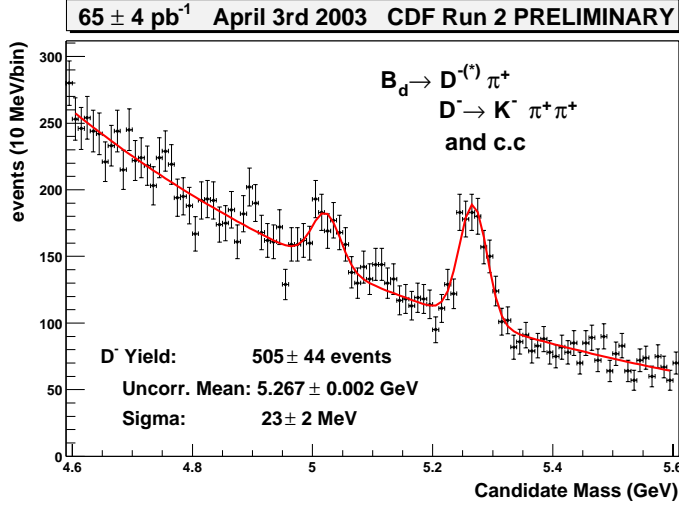


Figure 2: Invariant mass distribution of $B_d \rightarrow D^\mp \pi^\pm$, with the D^{*-} visible on the left.

5 $B_s \rightarrow D_s^\mp \pi^\pm$

The selection requirements for the $B_s \rightarrow D_s^\mp \pi^\pm$ signal are identical to the $B_d \rightarrow D^\mp \pi^\pm$ normalisation mode, except for the L_{xy} cuts³ on the B_s and D_s , and an invariant mass cut on the ϕ from the D_s ($D_s \rightarrow \phi\pi$)⁴. The invariant mass distribution obtained can be seen in figure 3. As with the $B_d \rightarrow D^\mp \pi^\pm$ mass plot, the excited charm-meson state can be seen on the left hand side of the plot. The systematic uncertainties of the analysis are summarized in table 1. The branching ratio result is then:

$$\frac{f_s \times BR(B_s \rightarrow D_s^\mp \pi^\pm)}{f_d \times BR(B_d \rightarrow D^\mp \pi^\pm)} = 0.42 \pm 0.11(stat) \pm 0.11(BR) \pm 0.07(syst) \quad (2)$$

where the systematic uncertainty from the external $B_d \rightarrow D^\mp \pi^\pm$ daughter branching ratio and the analysis are quoted separately. Using the PDG[4] measurement:

$$\frac{f_s}{f_d} = 0.273 \pm 0.034 \quad (3)$$

²where each $L_{xy}^X = \vec{P}_t^{xy} \cdot (\vec{X}_{xy} - \vec{X}_{PV})$ is calculated with respect to the primary vertex (\vec{X}_{PV}).

³ $L_{xy}^{D_s} > 400 \mu\text{m}$, $L_{xy}^{B_s} > 100 \mu\text{m}$

⁴ $m(K^+ K^-) \in [1.013, 1.028] \text{ GeV}$

the result becomes:

$$\frac{BR(B_s \rightarrow D_s^\mp \pi^\pm)}{BR(B_d \rightarrow D^\mp \pi^\pm)} = 1.61 \pm 0.40(stat) \pm 0.40(BR) \pm 0.26(syst) \pm 0.20 \left(PDG \frac{f_s}{f_d} \right) \quad (4)$$

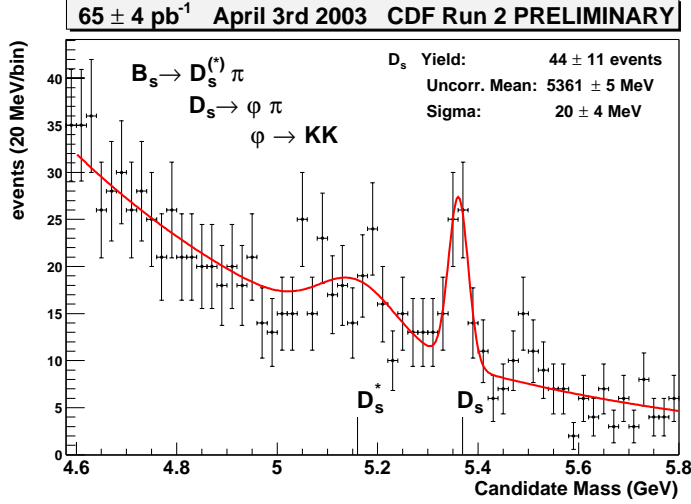


Figure 3: Invariant mass distribution of $B_s \rightarrow D_s^\mp \pi^\pm$, with the D_s^{*-} visible on the left.

Particle	$\sigma \left(\frac{N_{B_s}}{N_{B_d}} \right)$
B_s	± 0.008
B_d	± 0.008

Fit systematics

Source	$\sigma \left(\frac{\epsilon_{B_s}}{\epsilon_{B_d}} \right)$
XFT 1-miss[3]	$-0.00 +0.001$
Min b quark p_t	$-0.08 +0.00$
B lifetimes	$-0.02 +0.04$
D lifetimes	$-0.00 +0.04$
Total	$-0.08 +0.06$

Monte Carlo Systematics

Table 1: $B_s \rightarrow D_s^\mp \pi^\pm$ systematic uncertainties. The left table gives the contributions due to the fit for the number of events. The right table gives the contributions due to the Monte-Carlo calculation of the reconstruction efficiencies.

6 $\Lambda_b^0 \rightarrow \Lambda_c^\pm \pi^\mp$

As with the $B_s \rightarrow D_s^\mp \pi^\pm$ analysis, there is a trigger confirmation required on the offline tracks. The analysis cuts are then: $[p_t(P) > 2 \text{ GeV}]$; $[p_t(\pi \text{ from } \Lambda_b^0) > 2 \text{ GeV}]$; $[p_t(\Lambda_b^0) > 7.5 \text{ GeV}]$; $[p_t(\Lambda_c^\pm) > 4.5 \text{ GeV}]$; $[ct(\Lambda_b^0) > 225 \mu\text{m}]$; $[ct(\Lambda_c^\pm \text{ from } \Lambda_b^0) > -65 \mu\text{m}]$; $[\text{Impact-Par}(\Lambda_b^0) <$

$100 \mu m]$; [$2.265 < m(A_c^\pm) < 2.303$]. The signal invariant mass distribution obtained can be seen in figure 4. There are several different components to the unbinned likelihood fit shown. The red curve is the contribution from fully reconstructed B-decays with 4 daughters (like the signal).⁵ The sources of systematic error are given in table 2. The result is then:

$$\frac{f_{A_b^0} \times BR(A_b^0 \rightarrow A_c^\pm \pi^\mp)}{f_d \times BR(B_d \rightarrow D^\mp \pi^\pm)} = 0.66 \pm 0.11(stat) \pm 0.09(syst) \pm 0.18(BR) \quad (5)$$

where the systematic uncertainty due to the external A_c^\pm branching ratio measurement and the analysis systematics are quoted separately. Using the PDG[4] measurement:

$$\frac{f_{baryon}}{f_d} = 0.304 \pm 0.053 \quad (6)$$

the result becomes:

$$\frac{BR(A_b^0 \rightarrow A_c^\pm \pi^\mp)}{BR(B_d \rightarrow D^\mp \pi^\pm)} = 2.2 \pm 0.4(stat) \pm 0.3(syst) \pm 0.7(BR + FR) \quad (7)$$

where the last source of uncertainty is the combined effect of the external measurements of the A_c^\pm branching ratio and the production fraction ratio.

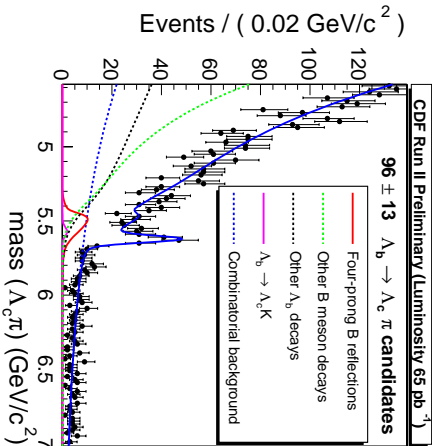


Figure 4: $\Lambda_b^0 \rightarrow \Lambda_c^\pm \pi^\mp$ invariant mass distribution

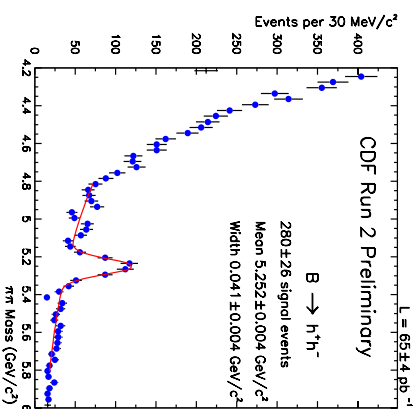


Figure 5: $B \rightarrow h^+ h^-$ invariant mass distribution

7 $B \rightarrow h^+ h^-$

The $h^+ h^-$ are required to be the trigger tracks. The analysis cuts are then: [$p_{T1} + p_{T2} > 5.5 GeV$]; [$|IP_{T1}|, |IP_{T2}| > 150 \mu m]$; [$2D$ -Flight-Dist(B) $> 300 \mu m]$; [$IP_B | < 80 \mu m]$; [Isolation⁶ > 0.5].

⁵This shape is calculated from monte-carlo, and the size of the contribution in the fit agrees with the amount of $B_d \rightarrow D^\mp \pi^\pm$ observed in the A_b^0 signal region.

⁶Defined in a cone about the B axis : $I = \frac{\sum_{B\text{-daughters}}(p_{Ti})}{\sum_{All\text{-Tracks}}(p_{Ti})}$ (calibrated on data).

	central value	variation range	(%) change
B^0 lifetime (μm)	462	457 – 467	± 0
Λ_b^0 lifetime (μm)	369	345 – 393	+4 – 5
Λ_c^\pm Dalitz structure	nonresonant		+1
p_t spectrum			+1
Λ_b^0 polarization	0	± 1	± 7
XFT[3]	2 miss	1 miss	+3
ϕ efficiency			+3
subtotal			± 9
Fit model(B^0)			± 6
Fit model(Λ_b^0)			± 8
$\frac{BR(\Lambda_c \rightarrow pk\pi)}{BR(D^+ \rightarrow K\pi\pi)}$	0	$\pm 27\%$	$\pm 27\%$

Table 2: Systematic uncertainties for the $\Lambda_b^0 \rightarrow \Lambda_c^\pm \pi^\mp$ BR measurement.

The invariant mass distribution obtained can be seen in figure 5, and a monte-carlo distribution of the various signal components is shown in figure 6. This plot underlines how essential particle-ID is to the analysis since the different signal contributions lie almost on top of each other⁷. The two forms of particle-ID employed are dE/dx and kinematic separation. While kinematic separation is less effective than dE/dx , it is still useful. The two event variables used are the invariant mass with the pion hypothesis, and the variable $\alpha = \left(1 - \frac{p_1}{p_2}\right) q_1$, where $p_{1,2}$ are the particle momenta, $p_1 < p_2$, and q_1 is the charge of the lower momentum particle. The more powerful dE/dx information is calibrated on a D^* sample where the bachelor π charge identifies which of the D^0 daughters is the K, and which is the π . A separation plot can be seen in figure 7. The systematic uncertainties of the $B \rightarrow h^+ h^-$ analysis are summarised in table 3.

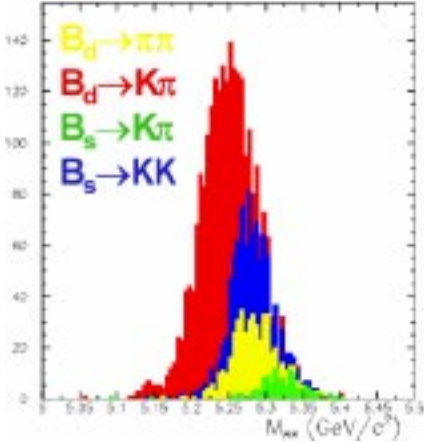


Figure 6: $B \rightarrow h^+ h^-$ MC distribution showing different signal components

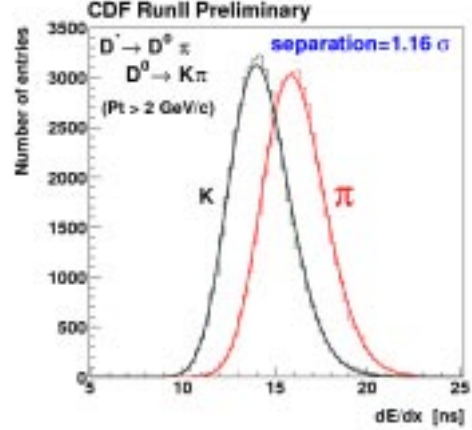


Figure 7: dE/dx separation for the D^* calibration sample.

⁷The $B \rightarrow \pi\pi$ and $B_s \rightarrow KK$ do in fact lie completely on top of each other.

The results are then:

$$\frac{BR(B_d \rightarrow \pi^\pm \pi^\mp)}{BR(B_d \rightarrow K^\pm \pi^\mp)} = 0.26 \pm 0.11(stat) \pm 0.055(syst) \quad (8)$$

$$A_{CP} = \frac{(\overline{B}_d^0 \rightarrow K^- \pi^+) - (B_d^0 \rightarrow K^+ \pi^-)}{(\overline{B}_d^0 \rightarrow K^- \pi^+) + (B_d^0 \rightarrow K^+ \pi^-)} = 0.02 \pm 0.15(stat) \pm 0.017(syst) \quad (9)$$

and a yield: $B_s \rightarrow K^\pm K^\mp = 90 \pm 17(stat) \pm 17(syst)$ events, showing an observation in this channel.

Effect	$\frac{BR(B_d \rightarrow \pi\pi)}{BR(B_d \rightarrow K\pi)}$	$A_{CP}(B_d \rightarrow K\pi)$
Bck. shape	+0.019 - 0.015	+0.002 - 0.009
$M(B_d)$	+0.004 - 0.004	+0.0003 - 0.0003
$M(B_s)$	+0.006 - 0.005	+0.002 - 0.003
Mass width	+0.004 - 0.009	+0.006 - 0.005
MC stat.	+0.002 - 0.002	+0.007 - 0.007
dE/dx cal.	+0.05 - 0.05	+0.01 - 0.01
Total	0.055	0.017

Table 3: Systematic uncertainties for the $B \rightarrow h^+ h^-$ BR, and A_{CP} measurements. The dE/dx calibration dominates.

8 Conclusion

In conclusion, CDF has robust signals in the three channels: $\Lambda_b^0 \rightarrow \Lambda_c^\pm \pi^\mp$, $B_s \rightarrow D_s^\mp \pi^\pm$, and $B_s \rightarrow K^\pm K^\mp$. The first measurements of the $B_s \rightarrow D_s^\mp \pi^\pm$, and $\Lambda_b^0 \rightarrow \Lambda_c^\pm \pi^\mp$ relative branching ratios have been made, and the $B_s \rightarrow K^\pm K^\mp$ signal is a first observation⁸. These constitute exciting first steps in the CDF programme for B_s^0 and Λ_b^0 physics.

References

- [1] A. Bardi *et al.*, Nucl. Instrum. Meth. A **485**, 178 (2002).
- [2] R. Blair *et al.* [CDF-II Collaboration], FERMILAB-PUB-96-390-E.
- [3] R. G. Oldeman [CDF Collaboration], arXiv:hep-ex/0307027.
- [4] K. Hagiwara *et al.* [Particle Data Group Collaboration], Phys. Rev. D **66**, 010001 (2002).

⁸The measurement of $\frac{BR(B_d \rightarrow \pi^\pm \pi^\mp)}{BR(B_d \rightarrow K^\pm \pi^\mp)}$ validates the extraction procedure.